

Aerodynamic Effect of Bicycle Wheel Cladding – A CFD Study

ABIJITH.T¹, DHANASEKAR.V², PARTHIBAN.S^{3*}

^{1,2,3}DEPARTMENT OF AERONAUTICAL ENGINEERING,
DHANALAKSHMI SRINIVASAN COLLEGE OF ENGINEERING AND TECHNOLOGY TAMILNADU ,INDIA

ABSTRACT: An aerodynamic drag in a bicycle can originate through the rotation of wheels, addition of cladding on the wheels are impact of it. In the present work, the effect of cladding on the wheels in a bicycle and also predicted the percentage of cladding in the aerodynamic drag by using a CFD model. Solid works flow simulation is used for an external analysis of airflow by accurate in the bicycle or rider. The $k-\epsilon$ turbulence model for cladding percentage between nil to maximum (100%). The aerodynamic drag force is analyzed with decrease to increase in cladding percentage. These are observed in velocities at 6, 8, 10 m/s. There observed maximum decrease in drag coefficient range is 5.2 – 5.3% it is compared to bicycle without cladding.

KEYWORDS: AERODYNAMIC DRAG, DRAG COEFFICIENT, CLADDING , CFD , BICYCLE

I. INTRODUCTION

To overcome the aerodynamic drag, cyclists utilize the large amount of power experienced by them. Aerodynamic drag represent between 70% and 90% of the total resistance experienced by a cyclist riding a bicycle. To overcome this resistance is a third-order polynomial of the velocity of travel is the power required by the cyclist. The consideration of the power of a cyclist is limited and it increases the competitiveness of sports, so does the need to improve the design of equipment in order to achieve better levels of performance with the same effort. By reducing the aerodynamic drag these improvements in design can be made possible. The major source of drag in bicycle is rotation of wheels. By reducing the number of spokes is the drag created by conventional spoked wheels can be limited. Here strength and rigidity factors limit this ability. A number of studies have attempted to examine the aerodynamics of bicycle wheels, primarily through wind tunnel and field tests. Kyle and Burke (1984) Godo et al (2009) and Wickern et al (1997), through experimental analysis, they observed a considerable difference in the aerodynamic drag while noticed in rotating and stationary wheels. Sunter and Sayers (2001) analysis the power expended by eight different wheels and the differences in the aerodynamic drag, and the characteristics such as the tire diameter, width and profile. Karabelas and Markatos (2012) observed that the rotation of wheels significant increases the drag and side force, and an increase in the number of spokes also increased the axial drag and vertical force of the wheel. Jermy et al (2008) observed the power dissipated by the aerodynamic resistance for a range of bicycle wheels, found that rotational drag due to wheels comprised 10-15% drag experienced in the bicycle. Zdravkovich (1992), crane and Morton(2018), Greenwell et al (1995) and Tew and sayers(1999) conducted a experimental studies on a range of a bicycle wheels such as tri-spoke and disk wheels exhibited a considerable reduction in aerodynamic drag, upto 50% as compared to commercially utilized wheels. In this they analysed that the velocity of rotation did not have a large impact on the drag coefficient of a wheel. Dyer and Noroozi(2005) conducted field tests on nine different cycle wheels and found the power expanded with the traditional spoked wheel to be over 20% higher as compared to deep section wheels, also the full disk wheel was observed to expend the lowest power. Monte et al (2016) analyzed that non-spoked continuous wheels were aerodynamically advantageous and it exhibited the lower drag than discontinuous and spoked wheels. Barry et al (2012) compared the experimental results obtained for the range of wheels in a cycle only configuration with these obtained, when a rider was included in the analyses and it trends a significant impact on the drag area, suggesting the choice of wheels must not be based on the individual aerodynamic characteristics of the wheel alone, but also on bio-mechanic characteristics concerned with a rider. Petrone et al (2018) also applied a full scale methodology in the analysis of a cyclists riding a cycle with three different sets of spoked vehicles and a change of 3.7% to 9% in time required in competitive time trial conditions. Computational Fluid Dynamics (CFD) is a powerful tool used for increasing in regularity over the past 10years. Increased computational power has meant that complex CFD simultaneous can be conducted in formerly reclusive fields such as bio energy, micro fluids, nanofluid mechanics and acoustics. The cycling aerodynamics involves the study of the flow of the air across an external body, that is a bicycle, computational fluid dynamics can be used for analysis and conducted an experimental and computational analysis for the flow of air across a bicycle wheel and observed the CFD results to be good agreement with the wind tunnel results and the validating the use of CFD in the context. Schwab et al(2008) referred the computer model analysis to study the effect of cross winds on the dynamics and control of a bicycle. Also observed that the crosswinds adversely affect the stability of a bicycle and increase its tendency to its steer into the wind. Blocken et al

analyzed the impact of fender coverage angle on the drag experienced by a bicycle computationally and obtained an optimum angle to reduce drag. Yu et al (2018) observed the various computational methods for the study of wheel rotation and its concluded moving wall. Also moving reference frame methods were appropriate when aerodynamic drag was important. Mannion et al (2018) analysed the moving wall computationally, and also moving reference frame and sliding mesh approaches in the modeling of bicycle wheel rotation. Also observed results to be good concordance with CFD values. Hobeika and Sebben (2018) concluded that the moving reference frame method was appropriate for modeling wheel rotation independent of geometry. Ilea et al (2019) referred the impact of wheel rims on the aerodynamics of wheels. It observed that alloy rims performed better. Pogni and Petrone (2016) used CFD for the analysis of five-spoked wheels using the $k-\epsilon$ model for a range of yaw angles, and reported results of drag and side forces, observing deeper wheel rims offered greater aerodynamic advantages. In a bicycle wheel, the addition of cladding plays an important role in the reduction of aerodynamic drag force and drag coefficient. In substantial effect is the same as the power expended by the cyclist. On a survey of literature, it is observed that a computational or parametric analysis of the effect of cladding on these aerodynamic parameters of a bicycle is sparsely available. The current work is an attempt in this direction. In the existing study, analyses have been carried out in order to determine the frontal area, aerodynamic drag force and drag coefficient as a function of percentage cladding, using CFD analyses. The diameter of the cladding varies from 0% to 100% of wheel diameter with a difference of 10% between consecutive analyses. The impact of velocity has been studied by simulating at 6m/s, 8m/s and 10m/s.

II. METHODOLOGY

For some current studies, the CAD model is carried out. The geometry was meshed and grid independence test were performed. CFD analyses were performed on the mesh and results were validated by comparison of reported data. The validation model was then used for performing the parametric study.

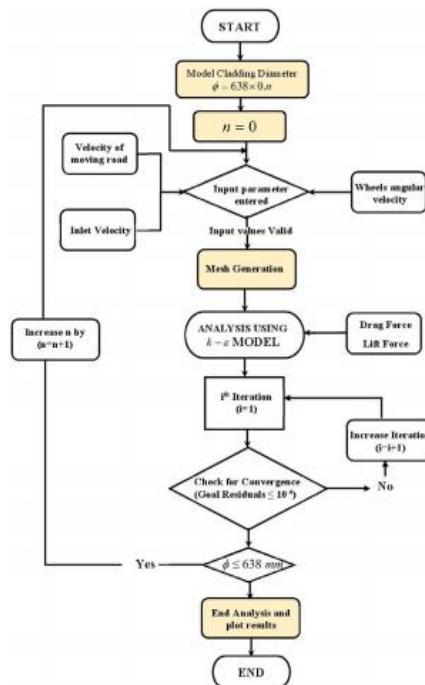


FIG.2.4.FLOW CHART OF ANALYSIS ALGORITHM

CAD MODEL

The 3D CAD model were assemble according to a standard city bicycle the bicycle frame, wheel (2 nos,32 spokes), cladding (2 nos), cyclist (a female of height 5ft 11in) helmet and solid plane under bicycle, representing the road. The cladding consists of two disks on the either side of a wheel. It present on both the front and back wheel. The center of cladding disks coincides with the center of wheel. It created using auto disk fusion 360 and solid works.

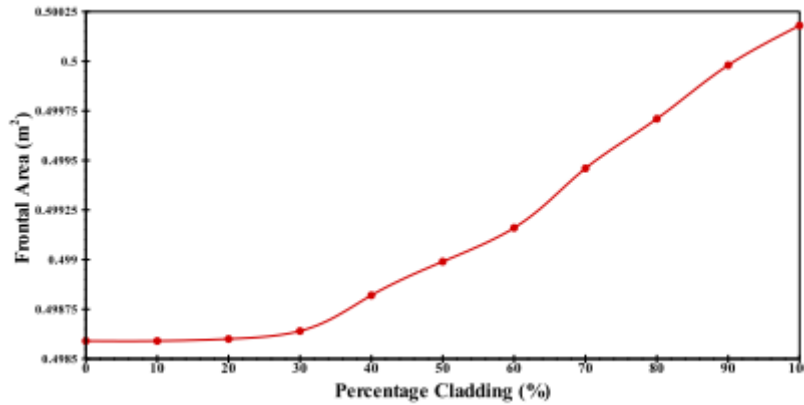


FIG.2.3.FRONTAL AREAS OF CAD MODELS AS A FUNCTION OF PERCENTAGE CLADDING

MATHEMATICAL MODELLING

Solid works flow stimulation was used for CFD analysis. The algorithm is used for the flow analysis. Flow stimulation for indirect time solver for approximation of convective/diffusive equation for low compressible flow. Defraeye et al (2010a) studied various turbulence model and also aerodynamic drag of a cyclist is most accurate predicted by k-ε model, as compared to corresponding wind tunnel. The k-ε turbulence models are used for current study. The analysis were governed by the 3D steady Favre Averaged Navier-Stokes (FANS) (Sobackin and Dumnov, 2013). Equation solved with second order accuracy using k-ε model (Jones and Launder, 1973). It discretized over the domain using finite volume method. Favre-averaging is it simplifies the average equations in significantly to density fluctuation of compressible flow. The finite-volume method attends the spatial discretization is performed. Reducing the error between the physical and computational coordinate system. The governing equations are

$$\partial p / \partial t + \partial (\rho u_i) / \partial x_i = 0$$

Where the ρ is the density of medium, t is the time, v is the velocity of flow, xi is the direction is represented by ui.

$$\partial (\rho u_i) / \partial t + \partial / \partial x_j (\rho u_i u_j) + \partial P / \partial x_i = \partial / \partial x_j (\tau_{ij} + \tau_{ij}) + S_i$$

Where P is the fluid pressure, τ_{ij} is shear stress tensor, S_i is the body force. A computational domain of length 32m, height 8m, width 8m. the road was modeled as a non-slip moving wall with velocity is equal to the relative velocity of travel of the bicycle of the air. The analyses were carried out with ambient temperature and pressure of 1bar and 298k. Inlet velocity of 6, 8 and 10m/s is applied as uniform velocity profile. On the downstream face is applied on ambient pressure outlet. On the upstream force have the computational domain. The wheels give rotational velocity corresponding to relative velocity of travel. The equation were the drag and lift coefficient the following are Solid works flow stimulation has a Cartesian meshing scheme. Advantage of a robust differential scheme are minimized the error and has greater speed (Sobachkinand Dum Nov, 2013). The mesh fineness is given by ratio factor. The factor ratio gives the size of the Cartesian mesh element. A greater ratio represents high fineness it containing the CAD model. The parametric study was carried out to find the effect of cladding percentage on the aerodynamic force and drag coefficient of a bicycle. The diameter of the cladding was varied between 0% to 100%, with the difference between consecutive analyses. The effect of velocity on the drag force and drag coefficient was studied by varying the velocity from 6m/s to 10m/s. convergence was monitored. The analyses was concluded when residuals of velocity components, continuity, k and ε reached an order of 10⁻⁶ as shown in figure. The results were tabulated post convergence and the next model was analysed.

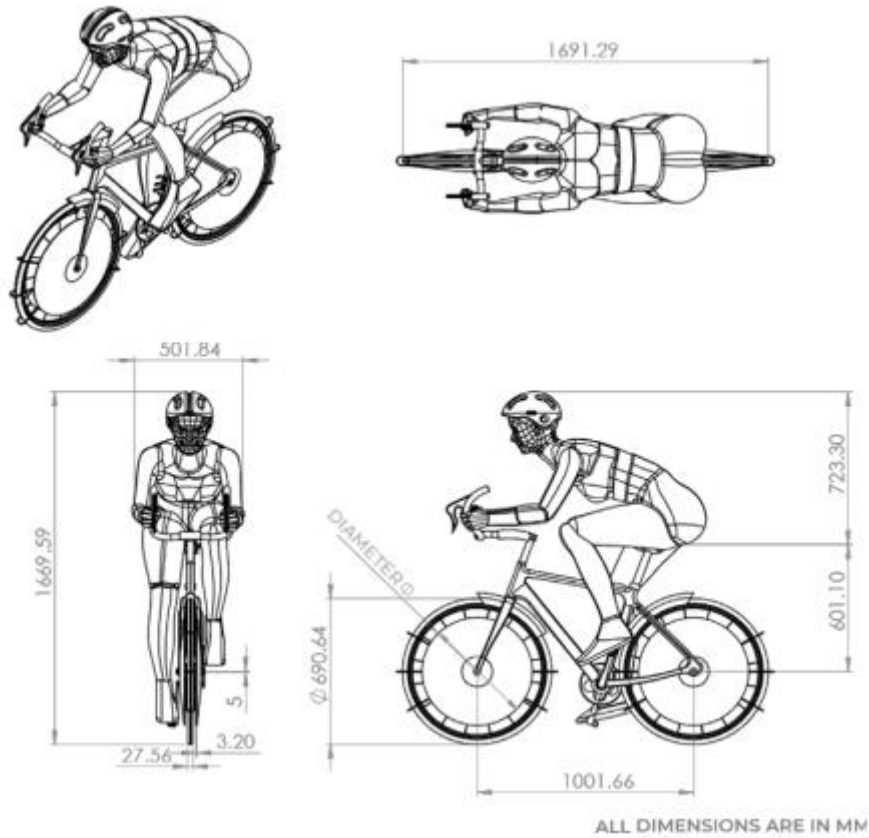


FIG.2.1. DIMENSIONS AND GEOMETRY OF BICYCLE AND CYCLIST

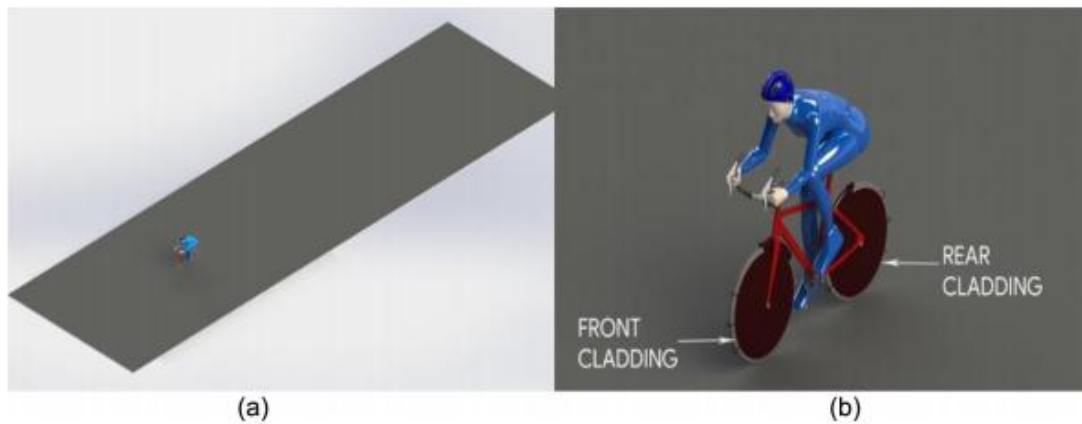


FIG.2.2. THE CAD ASSEMBLY USED IN THE ANALYSIS (A) WIDE ISOMETRIC VIEW (B) CLOSE-IN ISOMETRIC VIEW

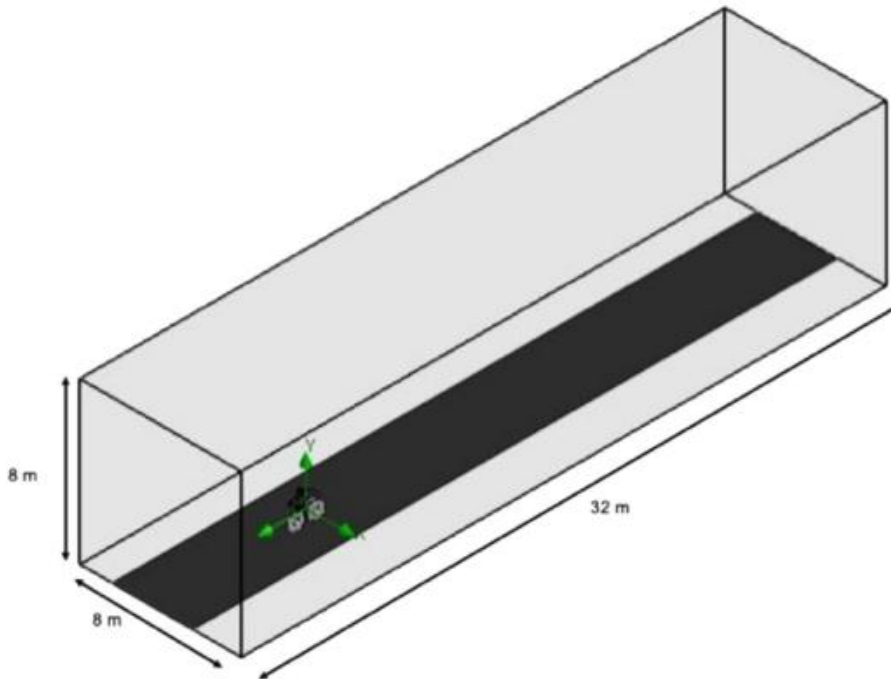


FIG.2.5. DIMENSIONS OF THE COMPUTATIONAL DOMAIN

TABLE 2.1

INPUT AND OUTPUT PARAMETERS

INPUT PARAMETERS CONDITIONS	OUTPUT PARAMETERS
Inlet: air velocity	Surface goal- drag force
Rotational velocity of bicycle wheels	Equation goal- drag coefficient
Velocity of solid plane(no slip moving wall)	Surface goal- lift force
Cycle- cyclist assembly: no-slip wall	Equation goal- lift coefficient
Outlet: ambient pressure	
Left, right and top walls: slip wall	

GRID INDEPENDENCE STUDY

To determine the grid size for the analysis. The value of the coefficient of drag is compared with ratio factor at mesh level 7. The mesh level of quantities the number of time is refined. Many times the mesh elements has been divided in the region of greater complexity. A mesh level of 1 means uniform mesh with equal dimensions, while increasing the refinement and increase in fineness of mesh.

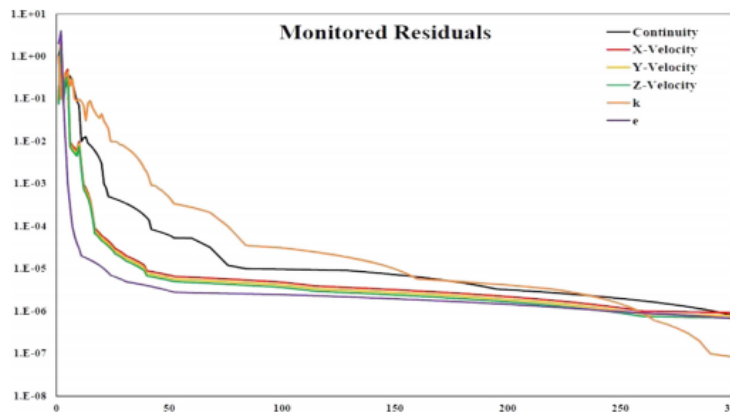


FIG: 2.6 RESIDUALS FOR CONVERGED SOLUTION OF BICYCLE WITHOUT CLADDING AT 6m/s

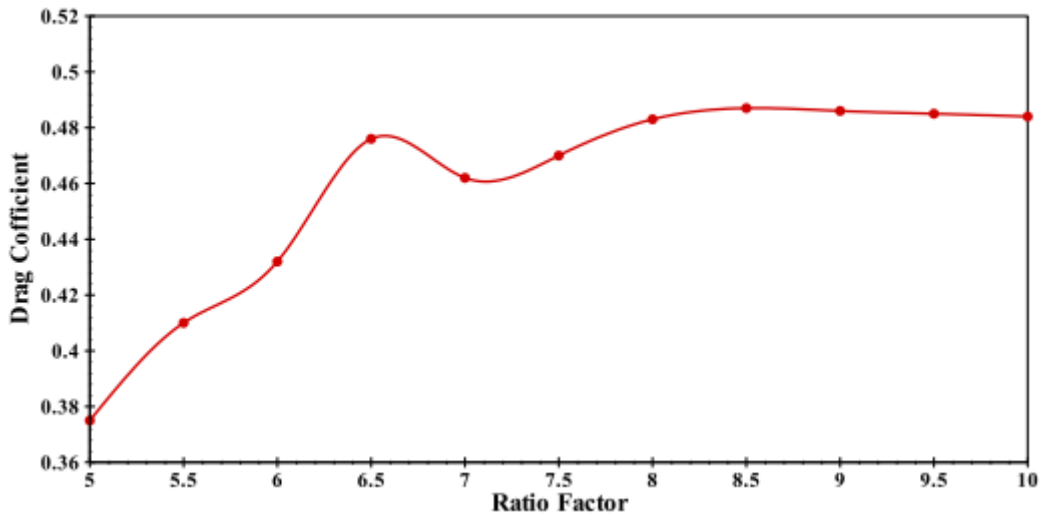


FIG.2.7. TREND OF DRAG COEFFICIENT WITH CHANGE IN RATIO FACTOR

The Cartesian mesh is important in region in close to model. The ratio factor of mesh between the aspect ratio. High ratio factor heads to finer and better quality close to model. Lower quality are away from it. This denotes saving in computational time without compromising on accuracy. It was conducted on the bicycle without cladding at 6m/s velocity with k-ε model. It beyond a ratio factor is 8.5, drag coefficient is minimal. Nine different line segment of front wheel on the rotating part. One-line passed through center and four each present on either side at equal interval. Each line segment has 11 points. Grid of mesh is 7 and ratio factor is 8.5, 9, 9.5, 10. Number of cells in the mesh ranges from 4×10^6 to 5×10^6 . Average element length has 0.7-0.8mm. The velocity in direction of travel (γ) was plotted as non-dimensional y-coordinate Y/Y_{max} it from origin. Maximum Y-coordinate has line segment under Y_{max} . All four mesh has mutual agreement. Increase in ratio factor increase in computational time. For this analysis ratio factor is 8.5

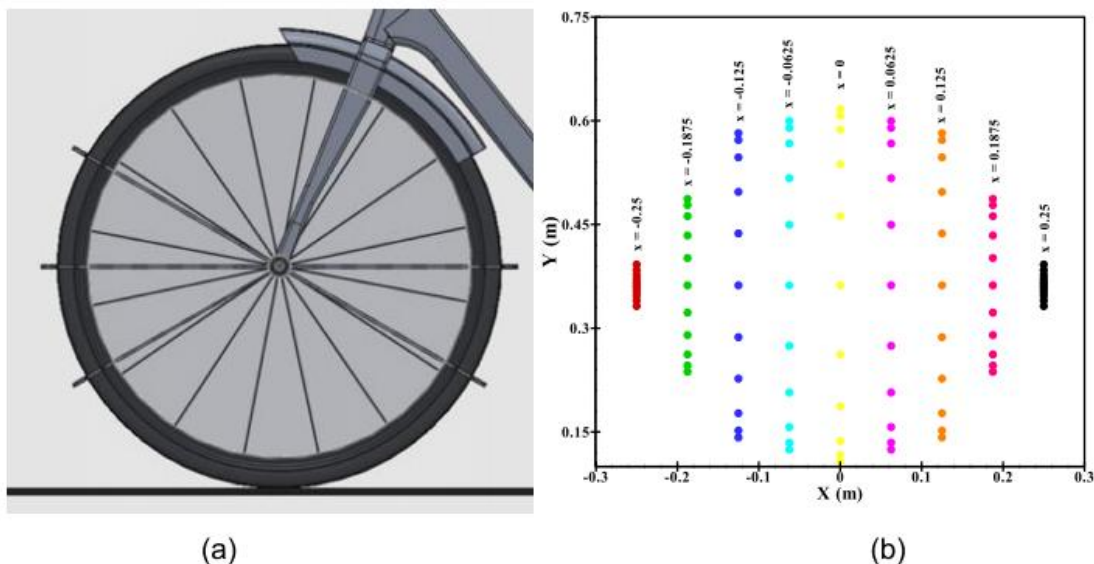


FIG.2.8 (A) REGION OF CAD MODEL STUDIED FOR MESH INDEPENDENCE (B) CARTESIAN COORDINATES OF POINTS

ANALYZED FOR THE MESH INDEPENDENCE STUDY

The ratio between the aerodynamic force and dynamic pressure. Drag area is used as a parameter both computational and experimental of bicycle. Drag area values are obtained by CFD analysis. Zdravkovich et al and Defraeye has done wind tunnel test for bicycle with current study and same velocities. Zdravkovich obtained average value of AC_d is 0.227, Defraeye et al obtained value 0.243. the drag area values in the current study there is no cladding in agreement with experimental value.

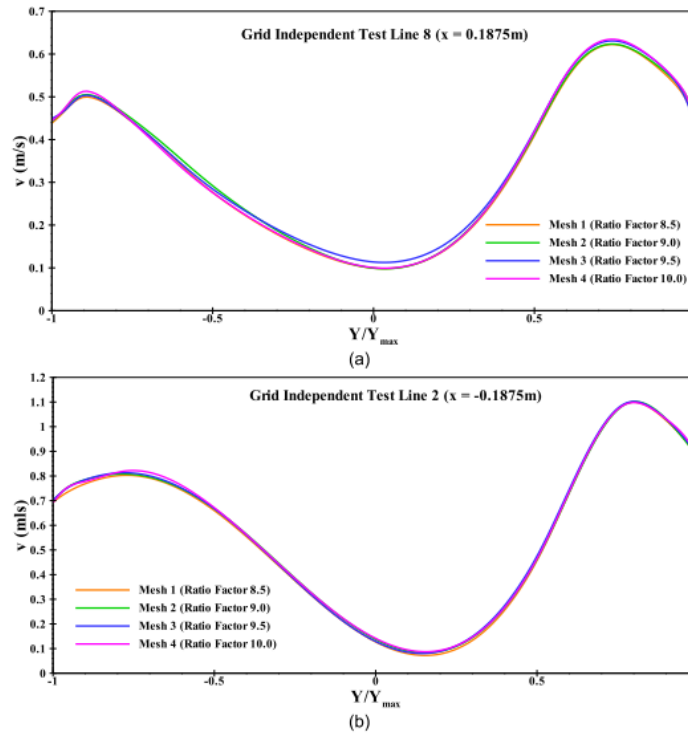


FIG.2.9. VELOCITIES FOR (A)LINE2 (B)LINES8 PLOTTED AGAINST 2-DIMENSIONAL Y-COORDINATE AT VARIOUS RATIO FACTORS

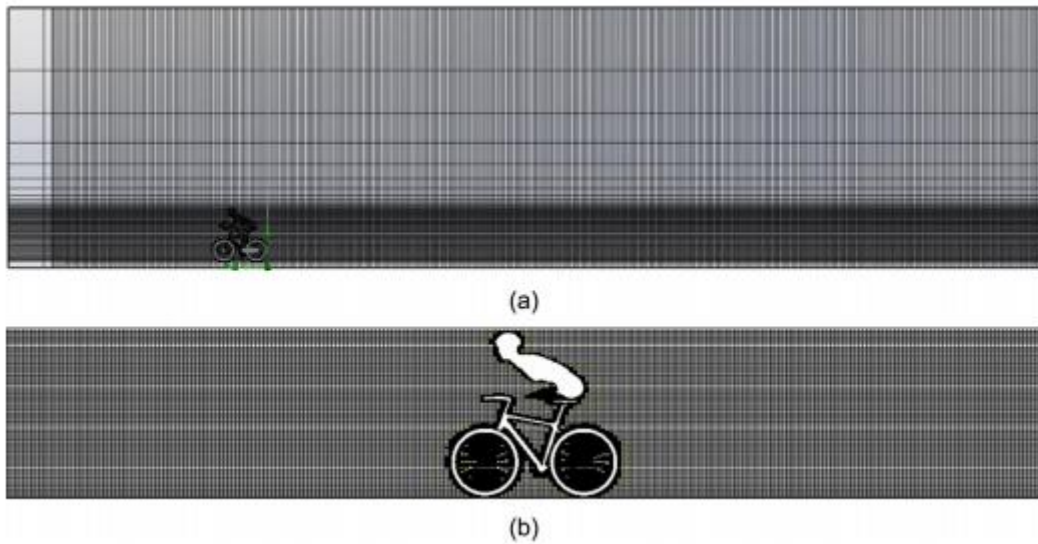


FIG.2.10. CARTESIAN MESH USED FOR ANALYSIS

**TABLE 3.1
DATA REPORTED IN PREVIOUS STUDIES AND OBTAINED IN CURRENT CFD ANALYSES**

STUDY	ACd(m2)	Zdrakovich et al. ACd(m2)	ERROR	Defraeye et.al.(2010) ACd(m2)	ERROR(%)
Current CFD study 10m/s	0.237	0.227	4.40%	0.243	2.47%
Current CFD study 8m/s	0.238	0.227	4.62%	0.243	1.64%
Current CFD study,6m/s	0.238	0.227	4.81%	0.243	1.50%

III. RESULT AND DISCUSSION

CFD analysis were used for drag force and drag coefficient as percentage cladding wheels at velocity of 6m/s, 8m/s, 10m/s. Fig.4.1 it represents velocity margin of the analysis at 10m/s velocity with 0% of cladding. Profile drag is experienced by a cyclist which have pressure differential. The complex geometry of cycle and cyclist creates the adverse angle of attack for inevitable air flow. The adverse pressure gradient causes separation of flow from the body. This flow is used to develop the wake behind the cycle and cyclist it creates the vortex. In the region of wake, it causes losses in pressure due to eddy formation it create low pressure. Increases in drag force by cycle and cyclist.

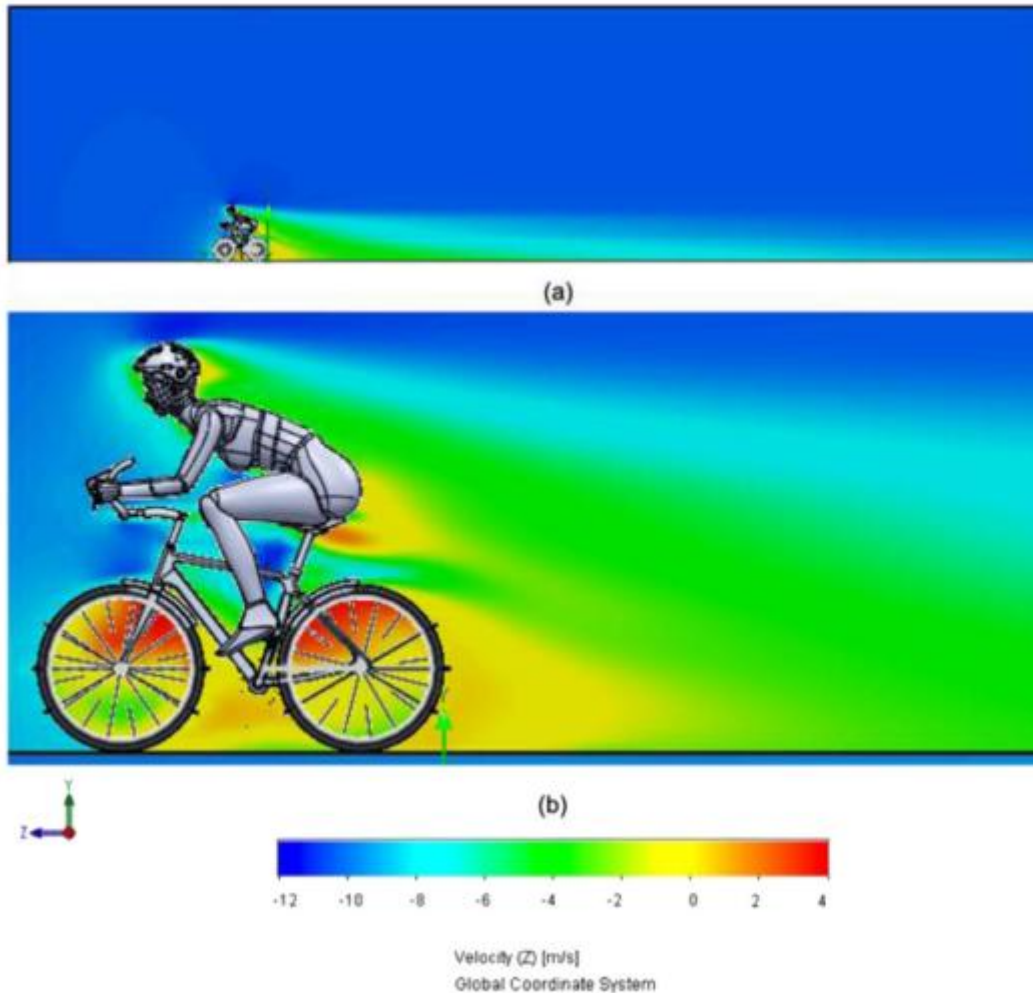


FIG.4.1 VELOCITY CONTOURS OF CFD ANALYSIS AT AIR VELOCITY OF 10m/s WITH 0% CLADDING

(a) WIDE VIEW (b) ZOOMED-IN-VIEW

FIG.4.2 depicts the turbulence intensity of cycle and rider at 0 to 100% cladding. It evident difference between the turbulence intensity behind the wheel. To decrease a low pressure created at a rear wheel and also decreases in drag by the cycle. In the turbulence flow, large amount of energy is dissipation by formation of eddy, it leads to loss pressure compare to laminar flow turbulence has greater contribute of drag. When the turbulence increases it has lower pressure in the development of drag force, which increases in drag.

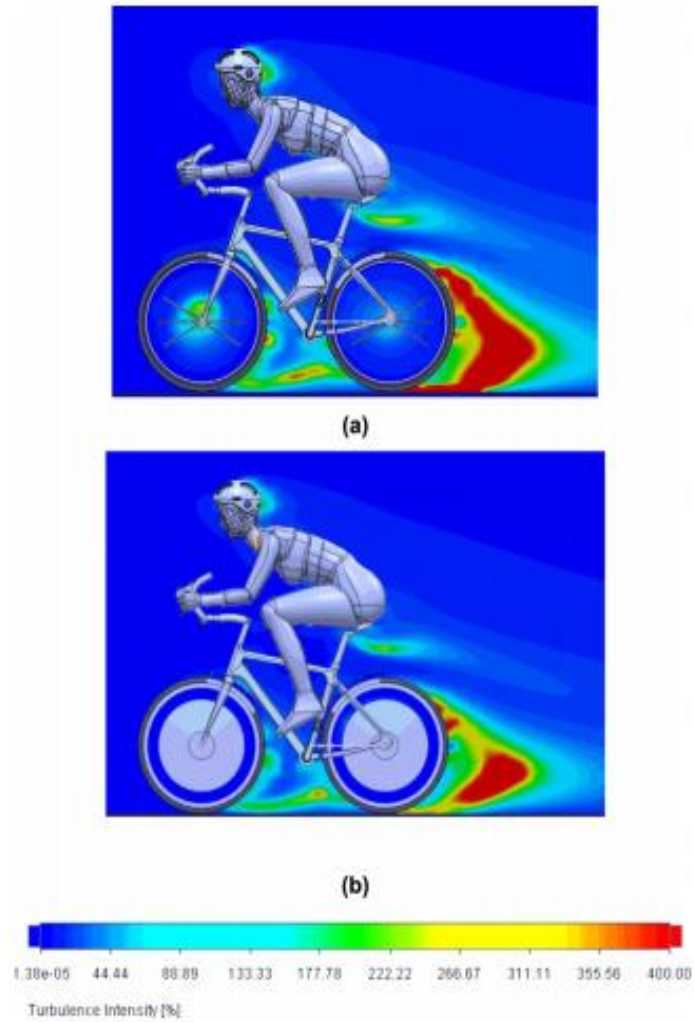


FIG.4.2 TURBULENCE INTENSITY CONTOURS FOR CFD ANALYSIS AT (a) 0% CLADDING (b) 80% CLADDING

FIG 4.3 the velocity streamlines for analysis the cycle at 5m/s with or without cladding. The reduction in turbulence, rotational velocity of air and irregular of vector in cycle with cladding also form small wake region. The pressure of cladding on the wheel provide air with lower exposure such wheel, spoke, towards flow separation. The reduction in flow separation formation of eddies and low pressure is reduced. This leads to vorticity and reduction in turbulence behind in te wheel and also reduction in drag force.

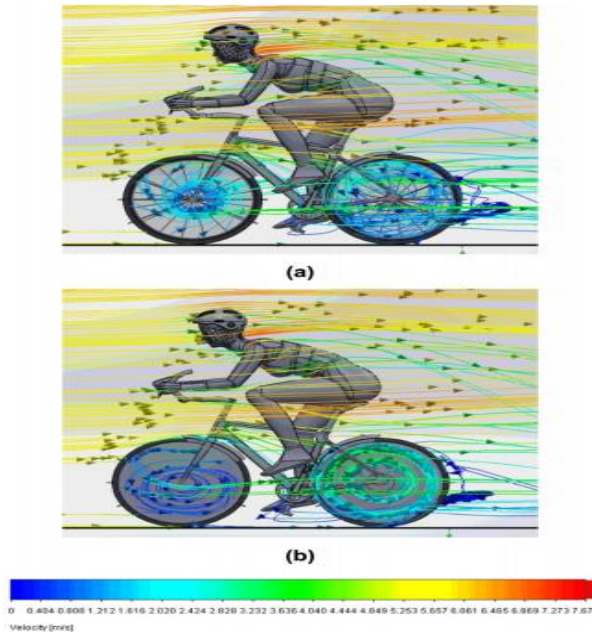


FIG.4.3 VELOCITY STREAMLINED AT VELOCITY 5m/s (a) 0% cladding (b) 100% cladding

FIG 4.4 represents the drag force as a function of the percentage cladding on the bicycle wheels. From the graph, it is evident that the drag force shows a similar decreasing trends for all velocities under consideration.

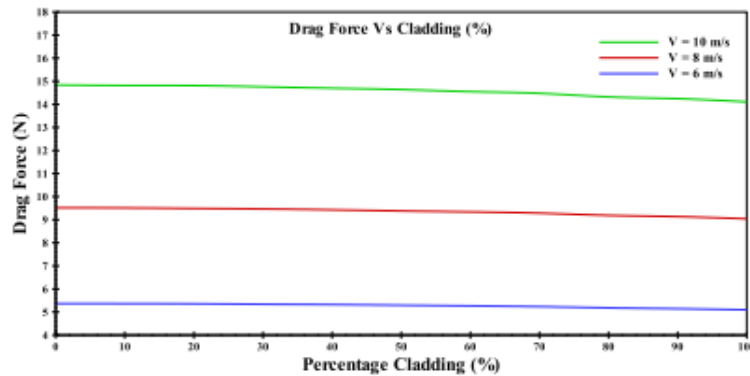


FIG.4.4 VALUES OF DRAG FORCE EXPERIENCED BY BICYCLE-CYCLIST ASSEMBLY AT THE ANALYZED VELOCITIES PLOTTED AGAINST PERCENTAGE CLADDING.

Fig.4.5 It represent the percentage change in drag force as compare to model without cladding. All three velocity decrease in all model. Rotating cycle wheel was observed that wheel with cladding of low drag coefficient than wheel of spokes also division of flow around the wheel Rotation of wheel form creation of eddies it reduce drag. Change in velocity it has negligible impact on the reduction in drag force.

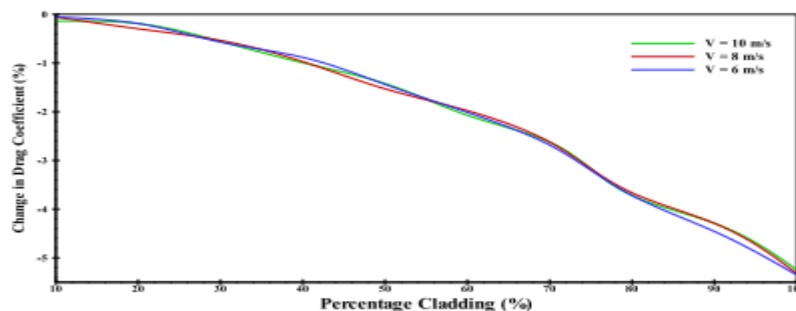


FIG.4.5. PERCENTAGE CHANGE IN DRAG FORCE AT THE ANALYSED VELOCITIES PLOTTED AGAINST PERCENTAGE CLADDING

Fig.4.6 it represents the drag coefficient of cladding percentage at air velocities at 6m/s,8m/s and 10m/s. all three velocities shows similar trends of decrease in drag coefficient . In the drag force the drag coefficient observe to decrease steadily with increase in cladding. The rate of reduction increase with increase in percentage cladding, the drag coefficient is increase with decrease in velocity. This denotes the research debraux et.al(2001) also drag area (ACd) was observed to decrease with increase in velocity .the velocities were between the range of the current study.

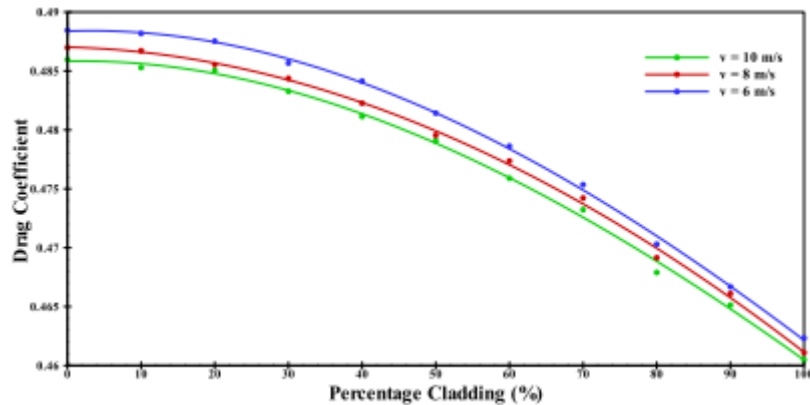


FIG.4.6 VALUES OF DRAG COEFFICIENT OF THE BICYCLE –CYCLIST ASSEMBLY AT THE ANALYZED VELOCITIES PLOTTED AGAINST PERCENTAGE CLADDING

Fig.4.7 It represents the percentage change in the drag coefficient as compared to the model without cladding. It is noticed in the case of drag force if the change in drag coefficient is similar in case of all three velocities. The minimum drag coefficient is observed at 100% cladding of all three velocities .the maximum reduction in drag coefficient is calculated as 5.3%, 5.3%, 5.2% for the case 6m/s, 8m/s and 10m/s respectively. The important conducted points of a reduction in turbulence to improve the aerodynamic of a cycle. Cladding on the wheels of a bicycle can go long way in reducing the aerodynamic drag of the bicycle in which the interest in city and competitive cycling, such as reduction in the drag produced by the cyclist can further lead to a reduction in time taken to ride the same distance also conservation of the energy consumed in drag. To determine the physical effects of the change in drag force. The virtual gain in the travel time is plotted as a function of cladding percentage. The percentage as shown in

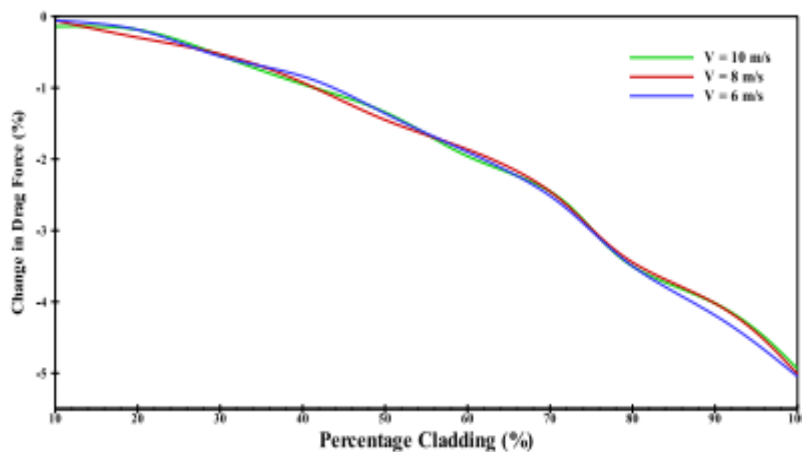


FIG.4.7. PERCENTAGE CHANGE IN DRAG COEFFICIENT AT THE ANALYZED VELOCITIES PLOTTED AGAINST PERCENTAGE CLADDING.

FIG.4.8.the gain is also calculated for the distance travelled of 1000m at the velocities stimulated. It shows from the figure the virtual travel time gained increases with increase in cladding percentage. The maximum gain varies from 23s for a travel velocity of 10m/s to 40s for a velocity of 6m.s. the decisions of competitive races hinge on margins of less than a second. To be mentioned that these are only virtual gains. The velocities during the race are always non-uniform and factor such as drafting ,track length and geometry airflow can change the actual time of travel.

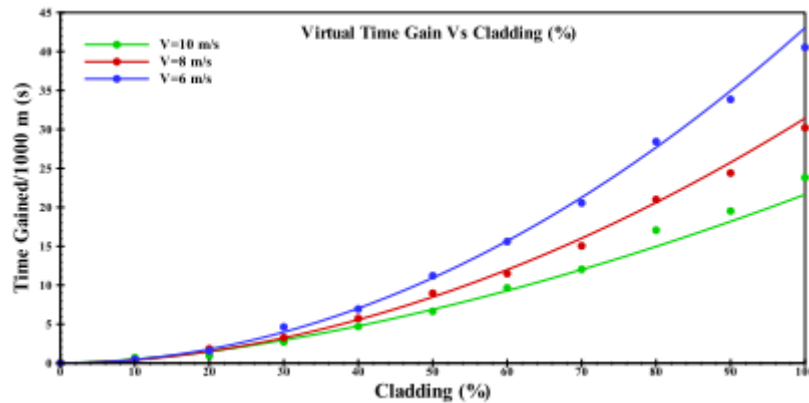


FIG.4.8.GAIN IN TRAVEL TIME PLOTTED AGAINST PERCENTAGE CLADDING

IV. CONCLUSION

3-dimensional CFD analysis were conducted by using solid work flow stimulation. To evaluate the impact of cladding on the aerodynamic drag and drag coefficient of a cyclist riding a bicycle. Analyses were perform from a percentage of cladding 0 to 100% at the velocities of 6, 8, 10m/s. so that the drag force and drag coefficient were decrease by increasing the cladding percentage. A maximum reduction in drag coefficient of 5.3%, 5.3%, 5.2% respectively at 6m/s, 8m/s, 10m/s of velocity. The addition of cladding over the bicycle is considerable with change in drag force as well as drag coefficient. By partially, lower cladding of wheels has effect on the drag coefficient than full cladding. While increasing in frontal area, the addition of cladding is marginal, so that the aerodynamic impact is large. Drag force and drag coefficient has decrease in value it forms high cladding percentage. Decrease in marginal for lower cladding percentage. This confirms the positive aerodynamic impact of cladding on the wheels of cycle. A reduction in drag coefficient and drag force it involves a reduction in effort on part of cyclist as well as reduction in time required for long distance travel.

REFERENCES

- [1]. Arora, B.B., 2014. Performance analysis of parallel hub diverging casing axial annular diffuser with 20° equivalent cone angle. Aust. J. Mech. Eng.<http://dx.doi.org/10.7158/m11-823.2014.12.2>.
- [2]. Asadollahi, A., Rashidi, S., Esfahani, J.A., Ellahi, R., 2018. Simulating phase change during the droplet deformation and impact on a wet surface in a square microchannel: An application of oil drops collision. Eur. Phys. J. Plus<http://dx.doi.org/10.1140/epjp/i2018-12135-6>.
- [3]. Barratt, M.J., 1965. The wave drag of a Hovercraft. J. Fluid Mech.<http://dx.doi.org/10.1017/S0022112065000563>.
- [4]. Barry, N., Burton, D., Crouch, T., Sheridan, J., Luescher, R., 2012. Effect of crosswinds and wheel selection on the aerodynamic behavior of a cyclist. In: Procedia Engineering.<http://dx.doi.org/10.1016/j.proeng.2012.04.005>.
- [5]. Blocken, B., Defraeye, T., Koninckx, E., Carmeliet, J., Hespel, P., 2013. CFD Simulations of the aerodynamic drag of two drafting cyclists. Comput. Fluids <http://dx.doi.org/10.1016/j.compfluid.2012.11.012>.
- [6]. Kashyap, V., Bhattacharjee, S., 2019. Computational analysis of flap Camber and ground clearance in double-element inverted airfoils. In: SAE Technical Paper Series.<http://dx.doi.org/10.4271/2019-01-5065>.
- [7]. Knupe, J., Farmer, D., 2009. Aerodynamics of high performance race bicycle wheels wing-light.de aerodynamics of high performance race bicycle wheels. Wing-light-de, Ger..
- [8]. Kyle, C.R., Burke, E., 1984. Improving the racing bicycle. Mech. Eng..
- [9]. Madhania, S., Muharam, Y., Winardi, S., Purwanto, W.W., 2019. Mechanism of molasses–water mixing behavior in bioethanol fermenter. experiments and CFD modeling. Energy Rep.<http://dx.doi.org/10.1016/j.egy.2019.04.008>.
- [10]. Mannion, P., Toparlar, Y., Blocken, B., Clifford, E., Andrienne, T., Hajdukiewicz, M., 2018. Analysis of crosswind aerodynamics for competitive hand-cycling. J. Wind Eng. Ind. Aerodyn.<http://dx.doi.org/10.1016/j.jweia.2018.08.002>.
- [11]. Mansour, M.A., Bakier, M.A.Y., 2015. Influence of thermal boundary conditions on MHD natural convection in square enclosure using cu–water nanofluid. Energy Rep.<http://dx.doi.org/10.1016/j.egy.2015.03.005>.

- [12]. Milani Shirvan, K., Ellahi, R., Mamourian, M., Moghiman, M., 2017a. Effects of wavy surface characteristics on natural convection heat transfer in a cosine corrugated square cavity filled with nanofluid. *Int. J. Heat Mass Transf* <http://dx.doi.org/10.1016/j.ijheatmasstransfer.2016.11.022>.
- [13]. Milani Shirvan, K., Mamourian, M., Mirzakhani, S., Ellahi, R., 2017b. Numerical investigation of heat exchanger effectiveness in a double pipe heat exchanger filled with nanofluid: A sensitivity analysis by response surface methodology. *Powder Technol* <http://dx.doi.org/10.1016/j.powtec.2017.02.065>.
- [14]. Monte, A.D., Leonardi, L.M., Menchinelli, C., Marini, C., 2016. A new bicycle design based on biomechanics and advanced technology. *Int. J. Sport Biomech* <http://dx.doi.org/10.1123/ijbs.3.3.287>.
- [15]. Pedley, T.J., 1997. Introduction to fluid dynamics. *Sci. Mar* <http://dx.doi.org/10.2307/j.ctvc77ddr.12>.
- [16]. Petrone, N., Giacomini, M., Koptug, A., Bäckström, M., 2018. Racing wheels' effect on drag/side forces acting on a cyclist at sportstech-miun wind tunnel. In: *Proceedings Vol. 2*, p. 210. <http://dx.doi.org/10.3390/proceedings2060210>.
- [17]. Pogni, M., Petrone, N., 2016. Comparison of the aerodynamic performance of five racing bicycle wheels by means of CFD Calculations. In: *Procedia Engineering* <http://dx.doi.org/10.1016/j.proeng.2016.06.192>.
- [18]. Rashidi, S., Akar, S., Bovand, M., Ellahi, R., 2018. Volume of fluid model to simulate the nanofluid flow and entropy generation in a single slope solar still. *Renew. Energy* <http://dx.doi.org/10.1016/j.renene.2017.08.059>.
- [19]. Rashidi, S., Esfahani, J.A., Ellahi, R., 2017. Convective heat transfer and particle motion in an obstructed duct with two side by side obstacles by means of DPM model. *Appl. Sci* <http://dx.doi.org/10.3390/app7040431>.
- [20]. Sayers, A.T., Stanley, P., 1994. Drag force on rotating racing cycle wheels. *J. Wind Eng. Ind. Aerodyn* [http://dx.doi.org/10.1016/0167-6105\(94\)90094-9](http://dx.doi.org/10.1016/0167-6105(94)90094-9).
- [21]. Schwab, A.L., Dialynas, G., Happee, R., 2018. Some Effects of Crosswind on the Lateral Dynamics of a Bicycle. In: *Proceedings* <http://dx.doi.org/10.3390/proceedings2060218>.
- [22]. Sobachkin, A., Dumnov, G., 2013. Numerical basis of CAD-embedded CFD. In: *NAFEMS World Congress 2013*.
- [23]. Sunter, R.J., Sayers, A.T., 2001. Aerodynamic drag of mountain bike tyres. *Sport. Eng* <http://dx.doi.org/10.1046/j.1460-2687.2001.00070.x>.
- [25]. Swain, D.P., 1994. The influence of body mass in endurance bicycling. *Med. Sci. Sports Exerc* <http://dx.doi.org/10.1249/00005768-199401000-00011>.
- [27]. Tew, G.S., Sayers, A.T., 1999. Aerodynamics of yawed racing cycle wheels. *J. Wind Eng. Ind. Aerodyn* [http://dx.doi.org/10.1016/S0167-6105\(99\)00034-3](http://dx.doi.org/10.1016/S0167-6105(99)00034-3).
- [28]. Wickern, G., Zwicker, K., Pfadenhauer, M., 1997. Rotating wheels - their impact on wind tunnel test techniques and on vehicle drag results. In: *SAE Technical Papers* <http://dx.doi.org/10.4271/970133>.
- [29]. Yu, X., Jia, Q., Bao, D., Yang, Z., 2018. A comparative study of different wheel rotating simulation methods in automotive aerodynamics. In: *SAE Technical Papers* <http://dx.doi.org/10.4271/2018-01-0728>.
- [30]. Zdravkovich, M.M., 1992. Aerodynamics of bicycle wheel and frame. *J. Wind Eng. Ind. Aerodyn* [http://dx.doi.org/10.1016/0167-6105\(92\)90520-K](http://dx.doi.org/10.1016/0167-6105(92)90520-K).